

DEVELOPMENT OF HARDNESS IN A Fe- BASED NANO-COMPOSITE ALLOY

S. Ahmadi^{1, 2} and H. R. Shahverdi²

* sh.ahmadi@modares.ac.ir

Received: February 2014

Accepted: July 2014

¹ Materials and Biomaterials Research Center, Biomaterials Group, Tehran, Iran.

² Tarbiat Modares University, Faculty of Engineering, Department of Materials Engineering, Tehran, Iran.

Abstract: Achieving extreme hardness in the newly synthetic steel formed by converting from initial amorphous state to subse-quent crystalline structure –named as devitrification process- was studied in this research work. Results of TEM observa-tions and XRD tests showed that crystallized microstructure were made up four different nano-scale phases i.e., α -Fe, $Fe_{36}Cr_{12}Mo_{10}$, Fe_3C and Fe_3B . More, Vickers hardness testing revealed a maximum hardness of 18.6 GPa which is signifi-cantly harder than existing hardmetals. Detailed kinetic and structural studies have been proof that two key factors were contributed to achieve this extreme hardness; supersaturation of transition metal alloying elements (especially Nb) and also reduction in the structure to the nano-size crystals.

Keywords: Transmission electron microscopy (TEM); Nano composites; X-ray diffraction (XRD)

1. INTRODUCTION

"Devitrified nanostructured steels" achieving from initial glassy state have been attracted much attention during last decades because of their unique hardness [1]. The main approach to produce iron based nanocomposites is through solid /solid state transformation in which nanostructured steels are obtained from unstable initial amorphous structures by annealing process [2]. Indeed, this new class of steels was first developed by over-quenching from a metallic glass and then heat treating the glass precursor over its crystalli-zation temperature to devitrify it to a multiphase nan-crystalline structure [3, 4].

It is worth nothing that overquenched metallic glasses, existing in a supersaturated metastable condition, can be transformed to multi -phase crystalline structures when enough energy was supplied to overcome the energy barrier of the nucleation [5, 6]. During devitrification transformation a very high nucleation frequency occurs with limited grain growth resulting multiple nano -crystalline phases [7, 8].

Microstructural evaluation in these kinds of steels showed that nanosize phases i.e., $Fe_{36}Cr_{12}Mo_{10}$, Fe_3B , Fe_3C and α -Fe were nucleat-ed in the amorphous structures after annealing process [9]. It was also proof that by nucleating of mentioned

nanosize phases not only hardness and wear resistance but also abrasion and fretting re-sistance of the alloys were promoted erratically [10, 13].

Although several researches are devoted to characterization of extreme hardness steels achieving from bulk amorphous steels, there are only a few attempts toward the detailed studies of the crystallization kinetics of alloys. In this paper, we launched the research toward expanding the previous works by D. J. Branagan [14] and his co-workers to evaluate the key factors in developing nanostructured ultra-high hardness steels categorized at metal matrix nanocomposites. To facilitate this idea, chemical composition of the alloys was designed on the class of materials called hardmetals. In fact, in this research work effects of alloying process via transient elements (Nb, Mo, Cr) on hardening of Fe-based nanostructured alloys have been studied. In other words, achieving high hardness, more than 18 GPa, in a nanostructured Fe-based composite alloy was evaluated in the research.

2. METHOD AND MATERIALS

In this research study, thin ribbons prepared from as cast cube ingots were used for kinetic and hardness investigations. In fact, multi- component Fe- based alloy ingots were prepared in an arc

furnace with nominal compositions of $\text{Fe}_{50}\text{Cr}_{18}\text{Mo}_7\text{B}_{16}\text{C}_4\text{Nb}_5$. Pure iron (99.7 mass %), chromium (99.9 mass %), niobium (99.9 mass %), molybdenum (99.9 mass %), and crystalline B (99.5 mass %) were used in an argon atmosphere to produce ingots. To achieve fully amorphous structures, rapidly solidified thin ribbons with a thickness of about 60 μm were prepared by melt-spinning technique (wheel speed: 32 m/s). Then, amorphous ribbons were annealed under vacuum (10^{-3} torr) in a furnace above the crystallization temperatures as the annealing process to obtain nanostructured structures.

Philips XRD device with $\text{CuK}\alpha$ radiation (voltage: 40 kV, amperage: 40 kA), equipped with X'pert software was used to identify crystallized phases. Composition of the ribbons was verified by using energy-dispersive X-ray spectroscopy. Moreover, microstructural evaluations were accomplished by a 200 kV JEOL transmission electron microscope equipped with an energy-dispersive X-ray spectrometer (INCA PentaFETx3-Oxford instruments). Before applying microstructural determination, samples were prepared in foil shape with 3 mm diameter. These discs were electro-polished in twin jet electro polisher with a solvent composed of 25% nitric acid and 75% methanol.

Vickers microhardness measurements were done with a 30 g load on the cross section of the samples using a Reichert-Jung Micro Durmat 4000 E system. For each sample, 7 to 10 hardness indentations were made and then the average of the measurements was

reported. The average standard deviation for the hardness measurements of the ribbons was 0.385 GPa.

3. RESULTS AND DISCUSSION

3. 1. TEM Observations

In figure 1, XRD pattern of the alloy (after melt-spinning process) is shown. As can be seen clearly, there are no significant crystalline sharp peaks in the chart showing an amorphous structure (formed in the samples after melt-spinning process).

In figure 2 result of the X-ray diffraction test is shown determining crystallization of α -Fe and other crystalline phases in the structure of the alloy after annealing process. It is clear that after annealing process structure of alloy was consist of crystalline phases such as α -Fe, Fe_3C , Fe_{23}B_6 , Fe_3B and $\text{Fe}_{36}\text{Cr}_{12}\text{Mo}_{10}$. In fact multi-phase structure was given after the heat treatment.

In figures 3 to 6 microstructures of the alloy in amorphous and also crystalline states are shown.

Significantly no crystalline phases are detected in the amorphous state (figure 3). It is essential to mention that one of the most striking features of the Fe-based nanostructured alloys produced by heat-treating of a preliminary amorphous state is the distinct morphologies of the crystalline phases (i.e. α -Fe, Fe_3C , Fe_{23}B_6 , Fe_3B and $\text{Fe}_{36}\text{Cr}_{12}\text{Mo}_{10}$).

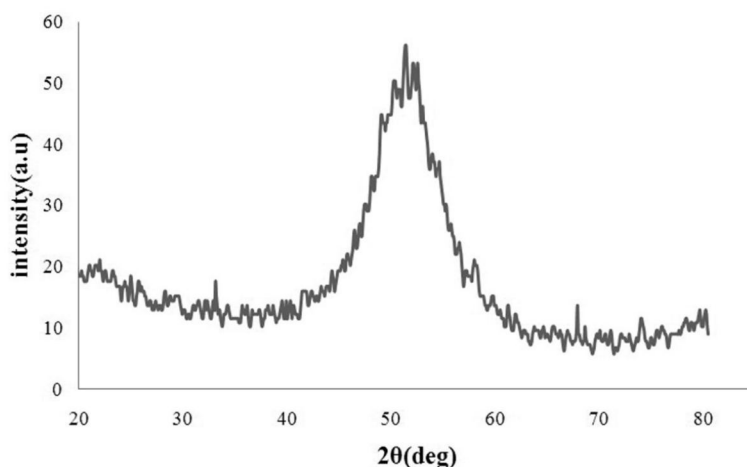


Fig.1. XRD pattern of $\text{Fe}_{50}\text{Cr}_{18}\text{Mo}_7\text{B}_{16}\text{C}_4\text{Nb}_5$ in amorphous state.

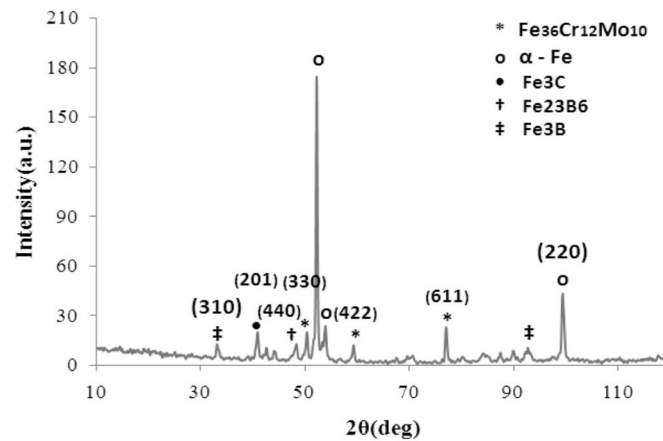


Fig. 2. XRD patterns of $\text{Fe}_{50}\text{Cr}_{18}\text{Mo}_7\text{B}_{16}\text{C}_4\text{Nb}_5$ alloy annealed at $850^\circ\text{C}/3\text{ h}$.

In the figures, microstructures of the alloy after heat-treating above the second crystalline temperature are shown. One can be seen that α -Fe crystals were formed in the structures of the alloys in mottled morphology. As mentioned earlier, unique features of crystalline phases can be effectively used toward identification of these nano-size phases. The nano scale phases crystallized in the structure of the alloy in special morphologies mentioned as following:

- i. α -Fe: mottled structure
- ii. Fe_3B : multi-twinned structure
- iii. Fe_3C : pentangle structure

- iv. $\text{Fe}_{36}\text{Cr}_{12}\text{Mo}_{10}$: layer (perlitic) structure

3. 2. Hardness Evaluation

Hardness measurements were taken on the cross section of both amorphous and heat treated ribbons; results are given in table 1. In figure 7, an example of the hardness identification on the cross section of a heat treated is shown. The as-cast ribbon exhibited high level of hardness of 13 GPa which become harder after heat treatment. Despite the similar alloys investigated by D. J. Branagan [14] and some other works [15, 16], in this new alloy amorphous samples show higher

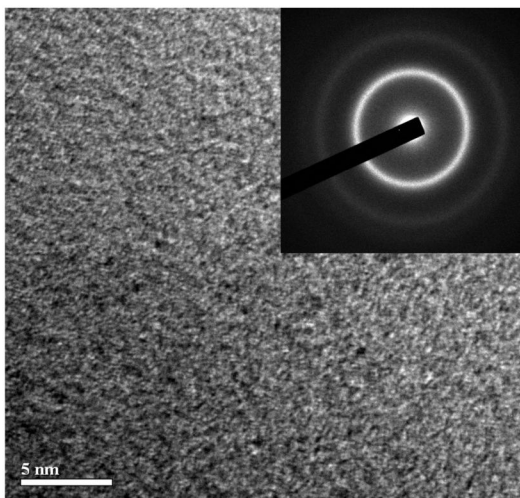


Fig. 3. Microstructure of $\text{Fe}_{50}\text{Cr}_{18}\text{Mo}_7\text{B}_{16}\text{C}_4\text{Nb}_5$ alloy in amorphous state.

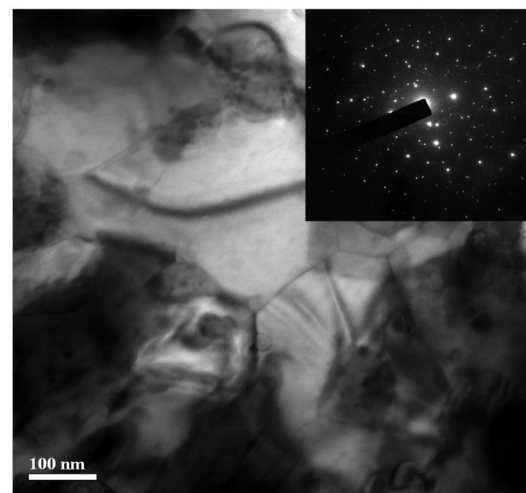


Fig. 4. Microstructure of $\text{Fe}_{50}\text{Cr}_{18}\text{Mo}_7\text{B}_{16}\text{C}_4\text{Nb}_5$ alloy in crystalline state.

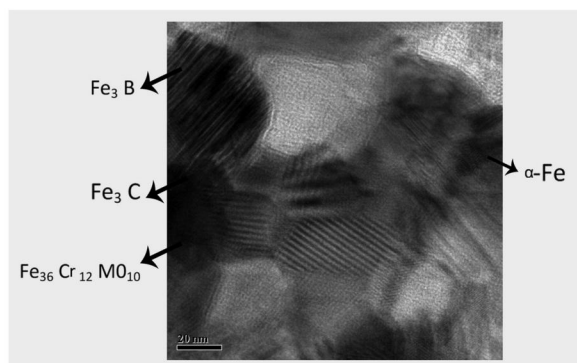


Fig. 5. Morphology of the crystalline phases in the structure of $\text{Fe}_{50}\text{Cr}_{18}\text{Mo}_7\text{B}_{16}\text{C}_4\text{Nb}_5$ alloy.

level of hardness that those of previous works. On the other hand, hardness significantly increases in the samples after heat treating but in the hard metals evaluated since now, similar observations have not been reported.

With respect to the crystallization of the nano-scale iron based phases, hardness mechanism in these nano-composite steel alloys are significantly different with that found in conventional steel alloys. In fact in the amorphous state, the key factor toward the extreme hardness is related to solid solution strengthening through non-equilibrium solid state. Due to the high amount of the alloying elements (i.e. Cr, Mo, Nb, and B) super saturated solid was formed during rapid quenching. In other words, super-saturations of the transition metallic elements near and above their equilibrium solubility limits are the first key factor in attending extreme hardness in amorphous state.

The second key factor toward obtaining high

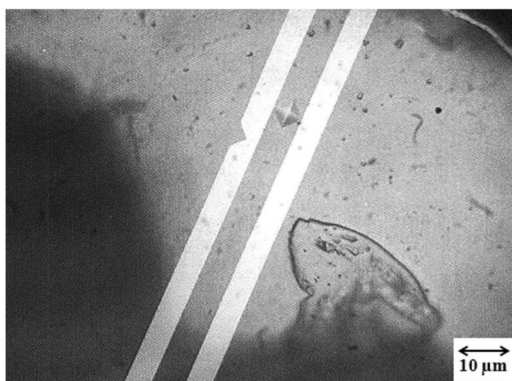


Fig. 7. Example hardness indentation on the cross section of a ribbon.

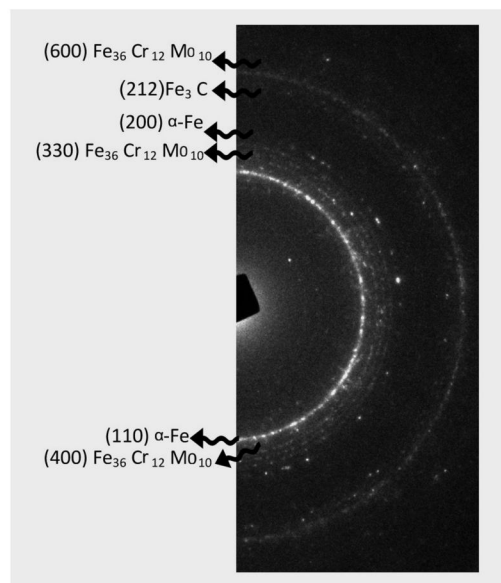


Fig. 6. Selected area diffraction pattern (SAD) for the ribbons heat treated at 850°C for 3 hours.

level of hardness is reduction of structure from amorphous solid to nano-crystalline solid. Indeed, hardness in the alloy was developed upon 18.6 GPa while crystal size decreased to about 50nm by heat treating over the crystallization temperature. By considering the data given in table 1, it can be inferred that forming super saturated solid (amorphous state) and then converting this solid to the crystalline structure consisting of the nano-size phases are the most effective mechanisms toward hardening of the alloy.

4. CONCLUSIONS

The hardness levels obtained by devitrification process in the alloy (18.6 GPa) are more than those of the similar hardmetals. Nb alloying is hypothesis as the key factor toward increasing hardness in both amorphous (by supersaturation of alloying elements e.g. Nb) and crystalline state (by reduction in the structure to the nanometer phases).

REFERENCES

1. Inoue, A., Shen, B. L., Koshiba, H., Kato, H., Yavari, A. R., " Ultra-high strength above 5000 MPa and soft magnetic properties of Co-Fe-Ta-B bulk glassy alloys ", *Acta Mater.* 52, 2004, 1631-1637.

Table 1. Results of hardness tests in the alloy

alloy	Hardness in amorphous state(GPa)	Hardness in crystalline state(GPa)	Average grain size(nm)
$Fe_{50}Cr_{18}Mo_7B_{16}C_4Nb_5$	13	18.6	50
$(Fe_{0.8}Cr_{0.2})_{79}B_{17}W_2C_2[18]$	11	16.2	150

2. Branagan, D. J., Breitsameter, M., Meacham, B. E. and Belashchenko, V., "High-Performance Nanoscale Composite Coatings for Boiler Applications", Journal of Thermal Spray Technology, ASM International, Volume 14(2), 2005, 196-204.
3. Pang, S. J., Zhang, T., Asami, K., Inoue, A., "Synthesis of Fe-Cr-Mo-C-B-P bulk metallic glasses with high corrosion resistance ", Acta Mater. 50, 2002, 489- 497.
4. Greer, A. L., "Metallic glasses on the threshold Materialstoday, 12, 2009, 14-22.
5. Branagan, D. J., Marshall, M. C., Meacham, B. E., "High toughness high hardness iron based PTAW weld materials", Materials Science and Engineering A, Vol. 428 , 2006, 116-123.
6. Nishiyama, N., Amiya, K., Inoue, A., "Novel applications of bulk metallic glass for industrial products Journal of Non- Crys. Solids, 353, 2007, 3615-3621.
7. Long, Z., Shao, Y., Xie, G., Zhang, P., Shen, B., Inoue, A., " Enhanced soft-magnetic and corrosion properties of Fe-based bulk glassy alloys with improved plasticity through the addition of Cr Journal of Alloys Compd. 462, 2008, 52-59.
8. Kappes, B. B., Meacham, B. E., Tang, Y. L., Branagan, D. J., " Relaxation, recovery, crystallization, and recrystallization transformations in an iron-based amorphous precursor", , Nanotechnology, 14, 2003, 1228-1234.
9. Ahmadi, S., Shahverdi, H. R. and Saremi, S. S., " Nano crystallization of α -Fe Crystals in Fe 52Cr18Mo7B16C4Nb3Bulk Amorphous Alloy ", Journal of Mater. Sci. Eng., 2011, 27(6), 497-502.
10. Ahmadi, S., Shahverdi, H. R., and Saremi, S. S., "In-vestigation of the Effects of Nb Alloying on Crystallization Kinetics of Fe55-xCr18Mo7B16C4Nbx(X=0,3)Bulk Amorphous Alloys ", Journal of Mater. Sci. Eng., 2011, 27(8), 735-740.
11. Ahmadi, S., Shahverdi, H. R., Afsari, M., Abdollah-zadeh, A., "Nano-Crystallization of Fe36Cr12Mo10 Phase in Fe55-xCr18Mo7B16C4Nbx (X=0, 3, 4) Amorphous alloys ", Journal of Non-cry. Solids, 365, 2013, 47-52.
12. Ahmadi, S., Shahverdi, H. R. and Saremi, S. S., "Kinetics of α -Fe Crystallization in Fe52Cr18Mo7B16C4Nb3 Bulk Amorphous Alloy ", Iranian Journal of Mater. Sci. Eng., Vol. 7, Number 4, 2010, 25-29.
13. Ahmadi, S., Shahverdi, H. R. and Saremi, S. S., "An Investigation toward the Nano-Crystallization of Fe55Cr18Mo7B16C4 Bulk Amorphous Alloy", Advanced Materials Research, Vols. 383-390 (2012) p p 3858-3862.
14. Branagan, D. J. and Tang, Y., "Developing Extreme hardness in Iron based Nanocomposite", Composites, PartA, Vol.33, 2002, 855-859.
15. Ahmadi, S., Shahverdi, H. R., " Nanocrystallization Mechanisms of Fe52Cr18Mo7B16C4Nb3 Bulk Amorphous Steel ", Iranian Journal of Mater. Sci. Eng., Vol. 10, Number 4, 2013, 1-7.
16. Ahmadi, S., Arabi, H., Shokuhfar, A., "Formation Mechanisms of Precipitates in an Al- Cu- Li- Zr Al-loy and their Effects on Strength and Electrical Resistance of the Alloy ", Journal of Alloys & compounds, 484, 2009.